Kinetics and Mechanism of Oxygen Exchange and Inversion along the M=O Axis in the Diprotonated and Monoprotonated Dioxotetracyanometalate Complexes of Re(V), Tc(V), W(IV), and Mo(IV)

Andreas Roodt,*[,1] Johann G. Leipoldt,[†,1] Lothar Helm,[2] Amira Abou-Hamdan,[2] and André E. Merbach*[,2]

Institut de Chimie Minérale et Analytique, Université de Lausanne, Bâtiment de Chimie (BCH), CH-1015 Lausanne, Switzerland, and Department of Chemistry, University of the Orange Free State, Bloemfontein 9300, South Africa

Received June 8, 1994[⊗]

Oxygen-17 NMR was utilized in aqueous medium (1.2−2.4 m KNO_3) to study the oxygen exchange kinetics in the *trans*-dioxotetracyanometalate complexes of Re(V), Tc(V), W(IV), and Mo(IV). The kinetics are described by the two-term rate law $R = (k_{aq}[MOH_2] + k_{OH}[MOH])/2$, where MOH_2 and MOH represent the di- and monoprotonated forms, $[MO(OH_2)(CN)_4]^{n-}$ and $[MO(OH)(CN)_4]^{(n+1)-}$, of the dioxotetracyanometalate complexes, respectively. The aqua complexes are by far more reactive toward exchange (k_{aq} values of $(9.1 \pm 0.1) \times 10^{-2}$ and (137 ± 5) s^{-1} at 25.0 °C for Re(V) and W(IV), respectively), compared to the $[MO(OH)(CN)_4]^{(n+1)-}$ ions under the same conditions (k_{OH}: Re(V), $(2.6 \pm 0.3) \times 10^{-3}$; W(IV), $(6.5 \pm 0.1) \times 10^{-4}$ s^{-1}), with the k_{OH} value for the Tc(V) hydroxo oxo complex at 25 °C obtained as 13 ± 1 s^{-1}. The activation parameters are as follows [$\Delta H^{\ddagger}$ (kJ mol^{-1}), $\Delta S^{\ddagger}$ (J K^{-1} mol^{-1})]. Re(V): k_{aq}, 84.00 ± 1, 16.91 ± 0.3; k_{OH}, 86.97 ± 6, -2.71 ± 20. W(IV): k_{aq}, 79.98 ± 2, 64.28 ± 7; k_{OH}, 79.49 ± 0.3, -39.30 ± 1. Tc(V): k_{OH}, 75.95 ± 4, 30.98 ± 15. No evidence was found for the dioxo complexes undergoing exchange unless protonated. A variable-temperature coordinated aqua line width study was done on the $[WO(OH_2)(CN)_4]^{2-}$ complex. The exchange data of the aqua complexes are in agreement with a dissociative activation, whereas the results obtained from the exchange of the hydroxo complexes point to a possible interchange/associative mechanism. This is the first case where data are obtained for substitution rates of the hydroxo ligand in these types of complexes. The four metal systems are correlated as a function of pH with regard to the (i) rate of inversion of the metal complex along the M=O axis, as manifested by the proton exchange, and (ii) oxygen exchange. These pH dependent plots enable the prediction of the inversion and oxygen exchange rates over more than a 10 order of magnitude range.

Introduction

The substitution and protonation behavior of the dioxotetracyanometalate complexes of Re(V), Tc(V), W(IV), and Mo(IV) has been extensively investigated the past decade[3] and has recently been reviewed.[4] We have in the course of these investigations selected these oxygen-containing complexes for a systematic study with regard to ligand, water, and proton exchange studies, using oxygen-17 and carbon-13 NMR for this purpose. Previous results are available for oxygen exchanoge on Re(V) dioxo complexes and related systems studied by oxygen-18 isotopic exchange.[5]

Scheme 1

$$[MO(OH_2)(CN)_4]^{n-} + H_2{}^*O \underset{}{\overset{k_{aq}}{\rightleftharpoons}} [MO(^*OH_2)(CN)_4]^{n-} + H_2O \quad (1)$$

$$K_{a1}\ -H^+ \downarrow\uparrow +H^+ \quad (2)$$

$$[MO(OH)(CN)_4]^{(n+1)-} + H_2{}^*O \underset{}{\overset{k_{OH}}{\rightleftharpoons}} [MO(^*OH)(CN)_4]^{(n+1)-} + H_2O \quad (3)$$

$$K_{a2}\ -H^+ \downarrow\uparrow +H^+ \quad (4)$$

$$[MO_2(CN)_4]^{(n+2)-} + H_2{}^*O \underset{}{\overset{k_O}{\rightleftharpoons}} [MO(^*O)(CN)_4]^{(n+2)-} + H_2O \quad (5)$$

We have already reported the characterization of these oxo complexes with NMR and were able to correlate chemical shifts and acid/base behavior with structural and infrared data.[6] The equilibria governing the oxygen and proton exchange in these systems are given by Scheme 1.

We have succeeded in determining the proton exchange rate constants in these complexes,[7] and therefore elucidating the mechanisms of the kinetics for the reactions shown in eqs 2 and 4, and showed that the proton exchange in these complexes

[†] Sadly, Professor Johann G. Leipoldt died during the preparation of this work.

[⊗] Abstract published in *Advance ACS Abstracts,* January 1, 1995.

(1) University of the Orange Free State.
(2) Université de Lausanne.
(3) (a) Roodt, A.; Leipoldt, J. G.; Deutsch, E. A.; Sullivan, J. C. *Inorg. Chem.* **1992**, *31*, 1080. (b) Roodt, A.; Leipoldt, J. G.; Basson, S. S.; Potgieter, I. M. *Transition Met. Chem.* **1988**, *13*, 336. (c) Roodt, A.; Leipoldt, J. G.; Basson, S. S.; Potgieter, I. M. *Transition Met. Chem.* **1990**, *15*, 439. (d) Potgieter, I. M.; Basson, S. S.; Roodt, A.; Leipoldt, J. G. *Transition Met. Chem.* **1988**, *13*, 209. (e) Purcell, W.; Roodt, A.; Basson, S. S.; Leipoldt, J. G. *Transition Met. Chem.* **1989**, *14*, 224. (f) Purcell, W.; Roodt, A.; Leipoldt, J. G. *Transition Met. Chem.* **1991**, *17*, 339. (g) Purcell, W.; Roodt, A.; Basson, S. S.; Leipoldt, J. G. *Transition Met. Chem.* **1989**, *14*, 369. (h) Roodt, A.; Basson, S. S.; Leipoldt, J. G. *Polyhedron* **1994**, *13*, 599. (i) Smit, J. P.; Purcell, W.; Roodt, A.; Leipoldt, J. G. *Polyhedron* **1993**, *12*, 2271. (j) Smit, J. P.; Purcell, W.; Roodt, A.; Leipoldt, J. G. *J. Chem. Soc., Chem. Commun.* **1993**, *18*, 1388.
(4) Leipoldt, J. G.; Basson, S. S.; Roodt, A. In *Advances in Inorganic Chemistry*; Sykes, A. G., Ed.; Academic Press: Tallahassee, FL, 1993; Vol. 40, p 242. (b) Leipoldt, J. G.; Basson, S. S.; Roodt, A.; Purcell, W. *Polyhedron* **1992**, *11*, 2277.
(5) (a) Toppen, D. L.; Murmann, R. K. *Inorg. Chem.* **1973**, *12*, 1611. (b) Murmann, R. K.; Robinson, P. R. *Inorg. Chem.* **1975**, *14*, 203.
(6) Roodt, A.; Leipoldt, J. G.; Helm, L.; Merbach, A. *Inorg. Chem.* **1992**, *31*, 2864.
(7) Roodt, A.; Leipoldt , J. G.; Helm, L.; Merbach, A. E. *Inorg. Chem.* **1994**, *33*, 140.

0020-1669/95/1334-0560$09.00/0

Scheme 2

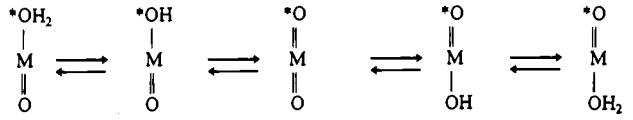

proceeds via protolysis, hydrolysis, and direct proton exchange. Furthermore, it was established that the enrichment of the oxo oxygen in both the $[MO(OH)(CN)_4]^{(n+1)-}$ and $[MO(OH_2)(CN)_4]^{n-}$ complexes proceeds *via* the dioxo species after rapid exchange between the bulk $H_2{}^*O$ and the coordinated aqua ligand, acting as "bottleneck" in the proton exchange process, as summarized in Scheme 2.

In this paper we describe the kinetics of the oxygen exchange of the complexes shown in Scheme 1 in reactions 1, 3, and 5, utilizing oxygen-17 NMR, and, furthermore, correlation of the results obtained with those of the previous proton exchange to describe the dynamic behavior of the coordination polyhedron upon protonation, as a function of pH.

Experimental Section

General Considerations. *Caution*: Technetium-99 emits a low-energy (0.292 MeV) β-particle with a half-life of 2.12×10^5 years. When this material is however handled in milligram amounts, it does not present any serious health hazard since ordinary laboratory glassware and other materials provide adequate shielding. Bremsstrahlung is not a significant problem due to the low energy of the β-particle emission, but normal radiation safety procedures must be used at all times, especially when handling solid samples, to prevent contamination and possible inhalation.

Preparation of Complexes and pH Measurements. $K_3Na[MoO_2(CN)_4]\cdot 6H_2O$, $K_3Na[WO_2(CN)_4]\cdot 6H_2O$, $K_3[TcO_2(CN)_4]$, and $K_3[ReO_2(CN)_4]$ were prepared as described previously.[3] Unless otherwise noted, all chemicals were of reagent grade, and all experiments were performed aerobically. A combined calomel electrode from Radiometer (GK2322C) and a Metrohm Herisau E603 pH-meter were calibrated with standard HNO_3 and decarbonated NaOH solutions in the usual way, incorporating the variation in the ion product of water as a function of both ionic strength and temperature.[8] Secondary buffers were also used for standardization at intermediate pH values, with the pH defined as $-\log [H^+]$. Some metal complex solutions were buffered by addition of citrate/MES (*N*-morpholineethanesulfonic acid) (for Re(V)) and borate/phosphate (Tc(V)). It was shown previously that these buffers showed no influence on the kinetics of these aqua oxo complexes in complex formation studies.[3,4]

NMR Measurements. The NMR experiments were done on Bruker AM-400 (cryomagnet 9.4 T), at 54.227 MHz (oxygen-17), and Bruker AMX-2 600 (cryomagnet 14.1 T), at 81.357 MHz (oxygen-17), spectrometers. The ^{17}O shifts were referenced to the water peak and measured with respect to the nitrate ion, $\delta(NO_3^-) = 413$ ppm, as internal reference. When necessary, the free water peak was also used as a quantitative reference for integration. All aqueous solutions used for oxygen-17 measurements contained 5% oxygen-enriched water. The temperature was controlled by a Bruker B-VT 1000 unit and was measured by substituting the sample tube for one containing a Pt-100 resistor.[9] The kinetic isotopic exchange studies were done on the 400 MHz instrument, where, unless otherwise stated in the figure headings, the parameters for the collection of ^{17}O NMR spectra were the following: a frequency range of 55.5 kHz was used to collect 2K data points with a pulse length of 15 μs and exponential line broadening of 80−100 Hz. The time between transients, of which between 1000 and 30000 were added prior to Fourier transformation, was 18 ms. The variable-temperature study on the W(IV) aqua oxo complex was done on the 600 MHz spectrometer over a temperature range of 273−306 K. The NMR parameters for this study were the following: a frequency range of 83.3 kHz was used to collect 8K data points applying the "1,−3,3,−1" pulse sequence (see "variable-temperature line broadening study on $[WO(OH_2)(CN)_4]^{2-}$"). An exponential line broadening of 25 Hz was used. The time between transients, of which 4K were added prior to Fourier transform, was 70 ms.

Kinetics and Data Treatment. The slow isotopic exchange in a chemical system, as for example for the reaction of a metal complex containing exchangeable oxygen ligands, can be followed by monitoring the bound oxygen-17 NMR signal growth as a function of time. For the kinetic runs a preweighed sample of the relevant metal complex was dissolved in thermostated ordinary water at the required pH, followed by the addition of an equivalent amount of 10% enriched ^{17}O water, introduction of the sample into a 10 mm NMR tube, and immediate commencement of the data collection. The formation rate of the dimeric species (only of importance in the Re(V) system), was always *ca.* 2 orders of magnitude slower than the oxygen exchange and did not affect the kinetic measurements. The fact that NMR was used enabled the selective monitoring of only the oxygen exchange on the monomeric species. All measurements were performed on solutions with total metal complex concentration of 0.2 m at ionic strength of 1.2−2.4 m (KNO_3 supporting electrolyte) unless otherwise stated. A selective variation of the metal complex concentration by a factor of up to 4 showed no influence on the kinetics in these systems.

The mole fraction, x, at time of sampling (directly proportional to the NMR signal height), of a coordinated oxygen-17 entity as a function of time, and at exchange equilibrium (x_∞) can be described by the exponential version of the MacKay equation, as has been shown previously.[10,11] The height h_b of an observed NMR signal corresponding to the coordinated oxygen-17 moiety in a specific complex can therefore be introduced in this function as in eq 6, where k represents the observed

$$h_b = h_{b\infty}[1 - \exp(-kt/(1 - x_\infty))] \quad (6)$$

exchange rate constant, h_b the height of the NMR signal at time of sampling, and $h_{b\infty}$ the height at exchange equilibrium. Equation 6 was used throughout this study for the determination of the exchange constant in the slow isotopic exchange experiments, where the mole fraction of the coordinated oxygen-17 at equilibrium was negligible (<0.01) and was consequently omitted in the exponential term.

A typical example of the signal increase observed with time for the Re(V) complex is shown in Figure 1, where the line represents the least-squares fit of the data to eq 6.

Results

General Results. In the previous study[7] we have reported ^{17}O signal characteristics as observed for these complexes, and it was shown that, in the absence of proton exchange, the different oxygen sites in the $[MO(OH_2)(CN)_4]^{n-}$, $[MO(OH)(CN)_4]^{(n+1)-}$, and the $[MO_2(CN)_4]^{(n+2)-}$ complexes span a range from *ca.* 1055 ppm (for the oxo signal of the Tc(V) aqua oxo complex) to −15 ppm (for the aqua signal of the W(IV) aqua oxo complex). It was also shown that the observed exchange at the oxo sites was a result of the fast proton exchange as shown in Scheme 2, where the dioxo complex acts as "bottleneck" for the proton exchange process. At lower pH values the oxo and the aqua/hydroxo signals are observed separately (slow exchange region with regard to *proton* exchange) and will combine at higher pH to give a coalesced signal, representing the average of the two specific sites (fast exchange region with regard to *proton* transfer). In the slow exchange regime, the oxygen exchange at each individual site with the bulk water can in principle be monitored. Similarly, in the fast exchange proton region, the isotopic oxygen exchange of the coalesced signal with the bulk can be monitored.

(8) Smith, R. M.; Martell, A. E. *Critical Stability Constants*; Plenum Press: New York, 1974; Vol. 4, p 1.
(9) Ammann, C.; Meier, P.; Merbach, A. E. *J. Magn. Reson.* **1982**, *46*, 319.
(10) (a) Helm, L.; Elding, L. I.; Merbach, A. E. *Inorg. Chem.* **1985**, *24*, 1719. (b) Helm, L.; Deutsch, K.; Deutsch, E.; Merbach, A. E. *Helv. Chim. Acta* **1992**, *75*, 210.
(11) Swaddle, T. W. *Adv. Inorg. Bioinorg. Mech.* **1983**, *2*, 121.

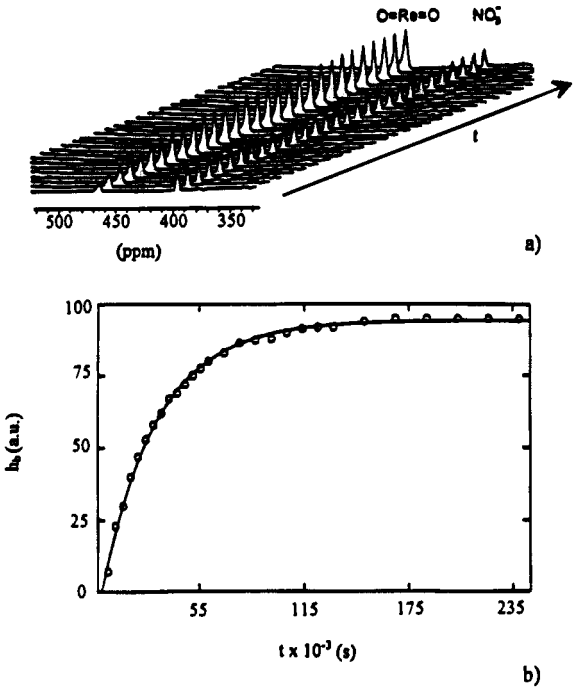

Figure 1. Slow isotopic exchange on the Re(V) center: (a) Oxygen-17 spectra showing signal growth *vs* time for $[ReO_2(CN)_4]^{3-}$; (b) least-squares fit of the data to eq 6. $[Re]_{tot.}$ = 0.2 m, pH = 6.6, T = 35.0 °C, and μ = 1.2 m (KNO_3).

A. Kinetic Studies on the Exchange between the NMR Coalesced Aqua/Hydroxo/Oxo Signal and Bulk Water Oxygen. Equations for Oxygen Exchange. The exchange equations of relevance in these metal complexes can in general be represented by eq 7, where $OMOH_2$, OMOH, and OMO

$$\left.\begin{matrix}OMOH_2\\OMOH\\OMO\end{matrix}\right\} + 2H_2O^* \underset{}{\overset{k_{obs}}{\rightleftharpoons}} \left.\begin{matrix}*OM^*OH_2\\*OM^*OH\\*OM^*O\end{matrix}\right\} + 2H_2O \qquad (7)$$

represent the $[MO(OH_2)(CN)_4]^{n-}$, $[MO(OH)(CN)_4]^{(n+1)-}$, and the $[MO_2(CN)_4]^{(n+2)-}$ complexes, respectively The pseudo-first-order rate constants, k_{obs}, were obtained by least-squares fits of the measured peak height increase of the relevant coalesced oxygen-17 signal to eq 6 as a function of time. The kinetics were studied by manipulation of $[H^+]$ in selected pH ranges, and strictly first-order kinetics were observed in all the runs.

The three different species in eq 7, where k_{aq}, k_{OH}, and k_O represent the oxygen exchange rate constants respectively as shown in eqs 1, 3, and 5, can in principle all undergo exchange, for which the overall rate law of the exchange is then given by eq 8. The concentrations of the different species in solution are

$$-d[M]/dt = k_{aq}[OMOH_2] + k_{OH}[OMOH] + k_O[OMO] \quad (8)$$

related through the acid dissociation constants, where [M] represents the total metal concentration. The overall rate law in eq 9 is obtained. Since there are two oxygen sites in every

$$-(d[M]/dt)/[M] = k_{aq}/(1 + K_{a1}/[H^+] + K_{a1}K_{a2}/[H^+]^2) + k_{OH}/(1 + [H^+]/K_{a1} + K_{a2}/[H^+]) + k_O/(1 + [H^+]/K_{a2} + [H^+]^2/K_{a1}K_{a2}) \quad (9)$$

complex in eq 7, the overall rate expression in eq 10 is obtained.

$$-(d[M]/dt)/[M] = 2k_{obs} \quad (10)$$

A combination of eqs 9 and 10 gives eq 11. If the dioxo

$$k_{obs} = \frac{k_{aq} + k_{OH}(K_{a1}/[H^+]) + k_O(K_{a1}K_{a2}/[H^+]^2)}{2(1 + K_{a1}/[H^+] + K_{a1}K_{a2}/[H^+]^2)} \quad (11)$$

complex does not undergo observable oxygen exchange, eq 11 can be simplified to eq 12 (see also discussion for Re(V) and

$$k_{obs} = \frac{(k_{aq} + k_{OH}(K_{a1}/[H^+]))}{2(1 + K_{a1}/[H^+] + K_{a1}K_{a2}/[H^+]^2)} \quad (12)$$

Tc(V)). Three distinct pH regions for the observed exchange rate constant, k_{obs}, can be identified according to eq 12. At low pH values where $[H^+] \gg K_{a1}$, eq 12 simplifies to eq 13.

$$k_{obs} = k_{aq}/2 \quad (13)$$

Similarly, at intermediate pH values, where $K_{a1} \gg [H^+] \gg K_{a2}$, eq 12 simplifies to eq 14. At high pH values, where $K_{a2} \gg$

$$k_{obs} = k_{aq}([H^+]/2K_{a1}) + k_{OH}/2 \quad (14)$$

$[H^+]$, eq 12 simplifies to eq 15. Table 1 gives a summary of

$$k_{obs} = k_{OH}([H^+]/2K_{a2}) \quad (15)$$

the oxygen-17 chemical shifts, acid dissociation constants, and complex formation rate constants (displacement of coordinated aqua by NCS^- ions) for the $[MO(OH_2)(CN)_4]^{n-}$ complexes for the Re(V), W(IV), Tc(V), and Mo(IV) metal centers. The proton transfer rate constants on the dioxo complexes are also reported therein.

Rhenium(V). The results from the ligand substitution studies show that the $[ReO(OH_2)(CN)_4]^-$ complex is the least reactive aqua oxo complex of the four metal centers with regard to complex formation. However, the half-life for the water exchange of the Re(V) aqua oxo complex at 25 °C, as calculated from these ligand substitution data, is still less than 10 s, which is too rapid to study by the conventional signal growth *vs* time technique. The concentration of the reactive aqua oxo can however be lowered substantially by simple pH increase to pH 2−5 (pK_{a1} value of $[ReO(OH_2)(CN)_4]^-$ complex = 1.31). The temperature and $[H^+]$ dependence of the exchange process, obtained by monitoring the coordinated oxygen-17 coalesced signal increase *vs* time, could indeed under these conditions be determined for the Re(V) and is given in Figure 2. The curve represents the least-squares fit (K_a values in Table 1 were used without compensation for possible temperature variation on values) of eq 12 to the data points. In Figure 2, it is also illustrated (dashed line) that eq 14 holds for the data when $K_{a1} \gg [H^+] \gg K_{a2}$ and eq 15 holds when $K_{a2} \gg [H^+]$. Note that the insert (a) shows a drawn line through the data points at high pH values, indicating a negligible k_O. The exchange rate constants for both the aqua oxo and hydroxo oxo complexes thus obtained are reported in Table 2, while the activation parameters, determined from the Eyring equation, are given in Table 3.

Tungsten(IV). The effect of temperature and $[H^+]$ on the oxygen exchange was studied for the W(IV) system by simple pH manipulation similar to the Re(V) mentioned above. In this case the pH however had to be varied around high values to enable the conventional peak height *vs* time data to be collected. The results are illustrated in Figure 3, where the solid lines represent the least-squares fit of eq 12 to the data. The values for the exchange rate constants for both the aqua oxo and hydroxo oxo complexes for tungsten(IV) are given in Table 2 while the activation parameters are reported in Table 3.

Table 1. Equilibrium and Kinetic Data for the Oxo Cyano Complexes of Re(V), Tc(V), W(IV), and Mo(IV) at 25 °C

param	metal center			
	Re(V)	Tc(V)	W(IV)	Mo(IV)
pK_{a_1}[a]	1.31 ± 0.07	2.90 ± 0.08	7.89 ± 0.05	9.88(5)
pK_{a_2}[a]	3.72 ± 0.05	4−5	14.5	16
k_{NCS}[b] (M^{-1} s^{-1})	0.0035	23	2.9	800
$\delta(^{17}O)$[c] (ppm)	440−462	578	345−355	435−440
k_{2a}[d] (M^{-1} s^{-1})	(1.1 ± 0.2) × 10^7	(1.1 ± 0.5) × 10^7		
k_{-2a}[d] (s^{-1})	(6 ± 1) × 10^{10}	(1.0 ± 0.4) × 10^{11}		
k_{2b}[d] (s^{-1})			(7 ± 2) × 10^8 [e]	(1.3 ± 0.2) × 10^9 [e]
k_{-2b}[d] (M^{-1} s^{-1})			(4 ± 2) × 10^8 [e]	(2 ± 1) × 10^7 [e]

[a] Reference 7. [b] Ligand substitution of aqua ligand in $[MO(OH_2)(CN)_4]^{n-}$ complex.[4] [c] Chemical shift of signal (in fast proton exchange region, and thus only one coalesced signal of oxo and hydroxo signals observed) monitored in kinetic study.[7] For Re(V) and Tc(V), isotopic exchange was also done by monitoring the signal of the dioxo complex; in the case of slow proton exchange the oxo signals of the aqua oxo complexes were monitored. [d] For the definition of the constants, see eqs 17 and 21. [e] The k_{2b} and k_{-2b} values were inverted in Table 2, ref 7.

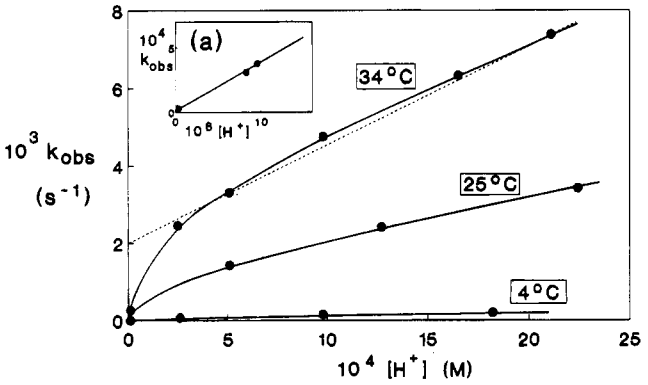

Figure 2. Temperature and pH dependence for oxygen exchange at the Re(V) center (μ = 1.2−1.5 m (KNO_3)). The insert (a) at 34.2 °C shows a line drawn through the three points at high pH which indicates a negligible k_O.

Table 2. Oxygen Exchange Rate Constants for Aqua Oxo and Hydroxo Oxo Complexes of Re(V), Tc(V), W(IV), and Mo(IV) Determined from ^{17}O Isotopic Exchange Studies at μ = 1.2−2.4 m (KNO_3) (Figures 2−4)

	temp (°C)	k_{aq} (s^{-1})	k_{OH} (s^{-1})
Re(V)	4.1	(6.6 ± 0.1) × 10^{-3}	(1.6 ± 0.1) × 10^{-4}
	25.2	(9.3 ± 0.7) × 10^{-2}	(3.4 ± 0.2) × 10^{-3}
	34.2	(2.6 ± 0.2) × 10^{-1}	(6.4 ± 0.9) × 10^{-3}
Tc(V)	8.1		1.8 ± 0.2
	25.0		15 ± 3
	35.0		32 ± 6
W(IV)[a]	6.1	14 ± 1	(6.9 ± 0.4) × 10^{-5}
	25.2	140 ± 3	(6.1 ± 0.03) × 10^{-4}
	32.7	301 ± 14	(1.51 ± 0.06) × 10^{-3}

[a] [H$^+$] calculated using K_w = 5 × 10^{-15}, 1.5 × 10^{-14}, and 2 × 10^{-14} at 6, 25, and 33 °C, respectively,[9] at 1.2 m ionic strength.

Of significance is the fact that the reactivity of the W(IV), Mo(IV), and Tc(V) systems toward water exchange could be estimated on the basis of the results from the Re(V) aqua oxo and hydroxo oxo complexes, postulating potential pH regions of reactivity toward oxygen exchange and confirmation of the postulated pH ranges by studying the slow observed exchange by conventional techniques. For tungsten(IV) a pH range of 12−14 was estimated, where exactly the same type of behavior as that observed for the Re(V) described above is expected, both the $[WO(OH_2)(CN)_4]^{2-}$ and the $[WO(OH)(CN)_4]^{3-}$ species undergoing exchange as described by eq 12.

Technetium(V). The $[TcO(OH_2)(CN)_4]^-$ complex is, as shown by the ligand substitution results in Table 1, more reactive than either the Re(V) or W(IV) systems. This, coupled with the fact that the binuclear species, $[Tc_2O_3(CN)_8]^{4-}$, is formed rapidly whenever there are appreciable amounts of the

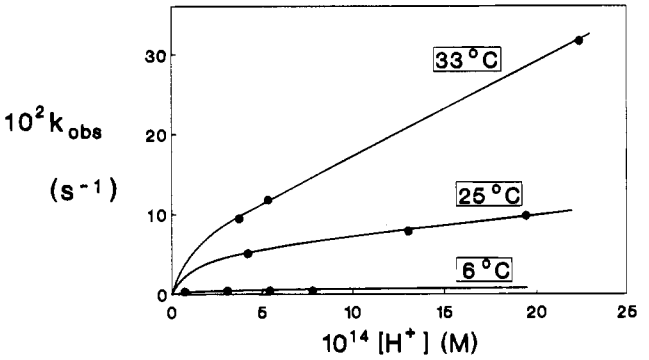

Figure 3. Temperature and pH dependence for oxygen exchange at the W(IV) center (μ = 1.4−2.4 m (KNO_3)).

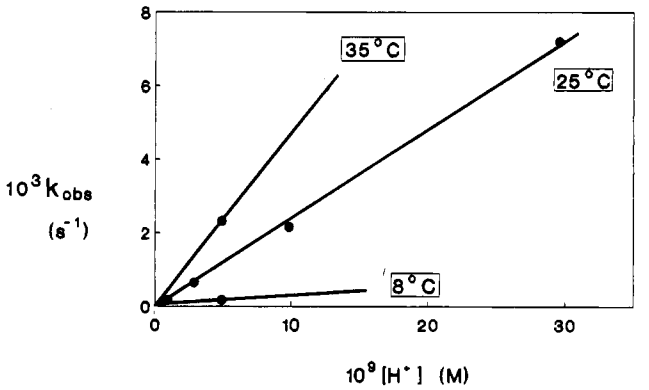

Figure 4. Temperature and pH dependence for oxygen exchange at the Tc(V) center (μ = 1.2 m (KNO_3)).

$[TcO(OH)(CN)_4]^{2-}$ complex present, *i.e.*, below pH *ca.* 5.5, prohibits any experiment around these acidities. However, at pH values around 7−9 the Tc(V) system could be adequately studied and the results are shown in Figure 4. A marked difference in the [H$^+$] dependence for the Tc(V) compared to the above mentioned Re(V) and W(IV) systems is however obvious. The origin of this stems from the fact that the Tc(V) was studied at pH values substantially higher than the pK_{a2} of 4 (K_{a2} ≫ [H$^+$]). Equation 15 consequently holds for this condition. Since there is an uncertainty in the value of pK_{a2} (estimated to be 4.5 from Table 1), there is also a corresponding uncertainty in that of k_{OH}, obtained from the slope of the lines in Figure 4. The exchange rate constants for the hydroxo oxo complex are reported in Table 2 while the activation parameters are given in Table 3.

Molybdenum(IV). The results from the complex formation reactions for the Mo(IV) aqua oxo complex compared to that of the other three metal centers showed the reactivity to be very high (Table 1). Similar pH manipulation to that of the W(IV)

Table 3. Oxygen Exchange Rate Constants (at 25 °C, μ = 1.2−2.4 m (KNO_3)) and Activation Parameters for $[MO(OH_2)(CN)_4]^{n-}$ and $[MO(OH)(CN)_4]^{(n+1)-}$

param	Re(V)	Tc(V)	W(IV)	Mo(IV)
k_{aq} (s^{-1})	$(9.1 \pm 0.1) \times 10^{-2}$	(500)[a]	137 ± 5	(4.1×10^4)[b]
$\Delta H^{\#}_{aq}$ (kJ mol^{-1})	84.00 ± 1		79.98 ± 2	
$\Delta S^{\#}_{aq}$ (J K^{-1} mol^{-1})	16.91 ± 0.3		64.28 ± 7	
k_{OH} (s^{-1})	$(2.6 \pm 0.3) \times 10^{-3}$	13 ± 1	$(6.5 \pm 0.1) \times 10^{-4}$	(0.2)[b]
$\Delta H^{\#}_{OH}$ (kJ mol^{-1})	86.97 ± 6	75.95 ± 4	79.49 ± 0.3	
$\Delta S^{\#}_{OH}$ (J K^{-1} mol^{-1})	-2.71 ± 20	30.98 ± 15	-39.30 ± 1	

[a] Estimated $k_{Tc} = 5000k_{Re}$; see text. [b] Estimated $k_{Mo} = 300k_W$; see text.

Table 4. Inversion Rate Constants (μ = 1.2−2 m (KNO_3)), As Determined from Isotopic Exchange at the Oxo Signal for the $[MO(OH_2)(CN)_4]^{n-}$ Complexes of W(IV) and Mo(IV)

metal	temp (°C)	pH	k_{inv} (s^{-1})
W(IV)	2.6	6.71	0.14 ± 0.05
	2.6	6.95	>0.47
Mo(IV)	2.6	7.78	$(3.3 \pm 0.2) \times 10^{-2}$
	4.3	4.55	$(8.8 \pm 0.7) \times 10^{-3}$
	4.5	5.13	$(4.4 \pm 0.3) \times 10^{-3}$
	4.5	5.81	$(5.1 \pm 0.6) \times 10^{-3}$
	10.2	6.60	$(4.0 \pm 0.4) \times 10^{-3}$

system proved to be *just* adequate to obtain one data point for the exchange reaction of the Mo(IV) system, at a very high basicity. The oxygen exchange study on the coalesced signal for Mo(IV) was done by the fast injection technique.[12] A prethermostated aliquot of enriched oxygen-17 water was injected into the thermostated buffered metal complex solution in the NMR tube, followed by immediate commencement of data acquisition. A rate constant of 0.0167(7) s^{-1} at 1.2 °C was obtained at $[OH^-]$ = 5 m. An attempt at 25 °C gave an approximate value of 0.14 s^{-1}.

B. Kinetic Studies on the Oxygen Exchange between the Oxo or Aqua Sites and the Bulk Water. As mentioned above, the oxygen exchange at the specific sites, *i.e.*, oxo or aqua ligand in the $[MO(OH_2)(CN)_4]^{n-}$ complexes, can also in principle be monitored providing the technique used is adequate for this purpose. The exchange of the aqua oxygen in these complexes is expected to be a rapid process and has to be monitored by more rapid measuring techniques than conventional isotopic exchange. This was achieved for the W(IV) aqua oxo complex by a variable-temperature line-broadening study as described below. The Mo(IV) could not be studied this way since the coordinated aqua signal could not be observed (very reactive metal center, see anation results in Table 1, in fast exchange with the bulk water signal).

Oxo Exchange in $[MO(OH_2)(CN)_4]^{2-}$ for M = W(IV) and Mo(IV). The exchange at the oxo site in the mentioned aqua oxo complex is a result of the proton exchange and consequent inversion processes shown in Scheme 2. It is governed by the concentration of the dioxo species. At low concentrations of this dioxo species (i.e., well below pK_{a2} for any of these metal centers) the oxygen exchange at the oxo site is a slow process and was successfully determined for both the W(IV) and Mo(IV) aqua oxo complexes at 2−10 °C by conventional isotopic exchange employing the fast injection technique, as described above. The pseudo-first-order rate constant for this inversion process, k_{inv} (see also discussion below), was in each instance obtained by a least squares fit of the data to eq 6. The results are reported in Table 4.

Variable-Temperature Line-Broadening Study on $[WO(OH_2)(CN)_4]^{2-}$. If a complex undergoes oxygen exchange too fast to be followed by conventional isotope labeling, as in the case of the coordinated aqua ligand of the W(IV) aqua oxo species, NMR line broadening as a function of temperature can be tried. In such a case, the transverse relaxation rate, $1/T_{2b}$, of the bound oxygen-17 nucleus is given by eq 16, where $1/T_{2Qb}$ represents the quadrupolar relaxation rate and k_{aq} the chemical exchange rate constant.

$$1/T_{2b} = 1/T_{2Qb} + k_{aq} \quad (16)$$

The ^{17}O signal of the bound water in the aqua oxo complex of W(IV) is observed at −15 ppm at pH values 5−6, where the $[WO(OH_2)(CN)_4]^{2-}$ complex is the only W(IV) species in solution. A variable-temperature study on the line width of this signal was undertaken in order to determine the water exchange constant, k_{aq} (eq 1), independently from the slow isotopic exchange study (Figure 3) at basic pH values. Paramagnetic relaxation agents such as $[Mn(H_2O)_6]^{2+}$, $[Gd(dtpa)(H_2O)]^{2-}$, $[Gd(edta)(H_2O)_n]^-$, and $[Dy(dtpa)(H_2O)]$ did not prove successful to effectively isolate the bound water signal, since the high concentrations of the anionic oxo cyano complexes employed resulted in either precipitation or decomposition in the presence of these agents. Instead, a selective pulse sequence on both the 9.4 and 14.1 T NMR spectrometers was used to isolate the bound water signal from the bulk. The following procedure was applied: The ^{17}O bulk water resonance suppression and the bound water resonance maximum excitation was done using a "1,−3,3,−1" sequence,[13] *i.e.*, 11.25°−*D*1−(−33.75°)−D1−33.75°−*D*1−(−11.27°)−ACQ, with $D1 = 1/(2\Delta\nu)$ ($\Delta\nu$ = chemical shift difference between the bulk and the bound water signals in Hz). The interpulse delay was set to 350 μs. This yielded ca. 970-fold depression of the bulk water signal relative to the bound water signal, as illustrated in Figure 5, showing spectra with and without (Figure 5a) the pulse sequence. The line-broadening results as a function of temperature, obtained from spectra as shown in Figure 5b, are reported in Table 5. Since the quadrupolar contribution to the observed signal was ca. 80−95%, with the water exchange (k_{aq}) contributing only 5−20% at the highest accessible temperature (only ca. 35 °C; complexes are very sensitive to decomposition at elevated temperature) in the line-broadening study, only an estimate of the exchange constant could be obtained, i.e., 50−200 s^{-1}.

Activation Parameters. The activation parameters reported in Table 3 were calculated from the temperature dependence data given in Table 2. In another calculation, all the individual data points (as illustrated in Figures 2−4) were introduced in a single least-squares analysis incorporating the Eyring equation and eq 12 (for Re(V) and W(IV)) or eq 15 (Tc(V)). The activation parameters and the k_{aq} and k_{OH} values thus obtained do not differ significantly from those reported in Table 3 but yielded a *ca.* 3- and 10-fold increase in the standard deviations for the $\Delta S^{\ddagger}$ and $\Delta H^{\ddagger}$ values, respectively. This is however not

(12) Bernhard, P.; Helm, L.; Ludi, A.; Merbach, A. E. *J. Am. Chem. Soc.* **1985**, *107*, 312.

(13) Hore, P. J. *J. Magn. Reson.* **1983**, *55*, 283.

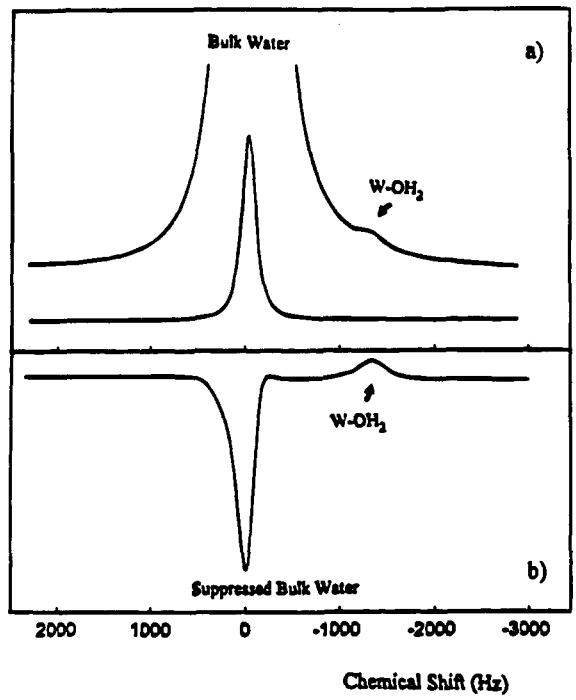

Figure 5. Oxygen-17 NMR spectra from a line-broadening study on the $[WO(OH_2)(CN)_4]^{2-}$ complex: (a) normal spectrum (note relative difference in bound and bulk water signals); (b) spectrum obtained with the "1,−3,3,−1" pulse sequence (see text) illustrating 3 order of magnitude depression of bulk water signal.

Table 5. Variable-Temperature Line-Broadening Study on Coordinated ^{17}O Aqua Signal in $[WO(OH_2)(CN)_4]^{2-}$ (NMR Parameters in Text)

temp (K)	$1/T_{2b}$[a] (s^{-1})	calcd[b] $1/T_{2Qb}$ (s^{-1})	k_{aq} (s^{-1})
275.5	1113	1035	
277.6	1007	1023	
280.8	985	1004	
283.1	971	990	
285.4	971	976	
288.7	962	957	
291.2	920	943	
294.4	919	924	
296.4	961	912	49
296.4	1046	912	134
299.6	1282	892	390

[a] Observed line broadening of bound aqua signal (see also Figure 5). [b] First six observed data points were used to calculate an average function for the quadrupolar relaxation as a function of temperature; the contribution of k_{aq} was calculated using eq 16.

unexpected since the variation of the individual pK_a values and pH measurements as a function of temperature is complex and could not be incorporated in all these calculations. Furthermore, the relative few data points used are expected to result in higher than normal standard deviations. Important however is the fact that similar values for the activation parameters and the exchange rate constants for the aqua oxo and hydroxo oxo complexes were obtained from both methods, providing additional confirmation that eqs 12 and 14 were indeed adequate to describe the observed exchange.

Discussion

Coordinated *vs* Bulk Oxygen Exchange. Rhenium(V) and Tungsten(IV). For the Re(V) system, Figure 2 (results at 34 °C) confirms the linearity as predicted by eq 14 (at intermediate pH values, i.e., $K_{a1} \gg [H^+] \gg K_{a2}$), showing that ordinary parallel reactions are observed by this conventional slow isotopic exchange study. Both the $[ReO(OH_2)(CN)_4]^-$ and $[ReO(OH)(CN)_4]^{2-}$ complexes are the only species in solution under these conditions and it is clear from eq 14 that the exchange of the aqua species (eq 1) is given by the slope and that of the hydroxo oxo (eq 2) complex by the intercept. The validity of eq 12 to describe the exchange kinetics over the wider pH range was verified by the determination of the observed exchange constants at pH values $\gg pK_{a2}$; see Figure 2 (results at 34 °C at low $[H^+]$). Under the latter conditions, a direct relationship between k_{obs} and $[H^+]$ was obtained (see also the results for the Tc(V) system, Figure 4). No evidence could under these conditions be found of the dioxo complex undergoing exchange; *i.e.*, an acid-catalyzed exchange is always observed when $K_{a2} \gg [H^+]$, as suggested by eq 15. This implies that eq 11 can be simplified and that the term containing k_O therein can consequently be eliminated, resulting in the two-term rate law as given in eq 12.

It is obvious that the W(IV) system behaves similarly to that of the Re(V); see Figure 3. Both eqs 12 and 14 were therefore adequate functions to determine the constants for the aqua oxo and the hydroxo oxo exchange pathways.

The Tc(V) system, on the other hand, is too labile with respect to water exchange to be monitored under the conditions of eq 14 applying, but the validity of eq 15 to define the exchange in this systems when $K_{a2} \gg [H^+]$ was consequently confirmed, again showing no indication of the dioxo complex undergoing observable exchange without acid catalysis; see also discussion below concerning the Tc(V) center. This observation is in agreement with oxygen-18[5a] isotopic exchange results reported for the Re(V) system, where a direct relationship between the observed exchange rate and the $[H^+]$ was found at pH values larger than pK_{a2}. In this specific study, only the k_{OH} value was determined but no explanation could be given for the results obtained at lower pH values, *i.e.*, the change to linearity of the k_{obs} *vs* $[H^+]$ function (Figures 2 and 3) at pH values lower than the pK_{a2} of the aqua oxo complex. This current NMR study however successfully accounts for all the observed behavior, allowing both the water exchange constant, k_{aq}, and the exchange constant for the hydroxo oxo complex, k_{OH}, to be determined; see Table 2. The k_{OH} value of 0.0342(5) s^{-1} at 35 °C determined by the above mentioned oxygen-18[5a] isotope study for Re(V) is in reasonable agreement with that obtained in this study (Table 2).

Molybdenum(IV). The complex formation results in Table 1 showed that the Mo(IV) aqua oxo complex is 2 orders of magnitude more reactive than the W(IV) complex. This was indeed observed, in line with the reasoning above with regard to reactivity as a function of pH for the Mo(IV). The results of this current study are in line with those obtained in a previous oxygen-18 isotopic exchange study.[5b] The authors reported the exchange rate constant for the $[MoO(OH)(CN)_4]^{3-}$ complex as >0.07 s^{-1} at 0 °C, which is in direct agreement with the observation from this current study. The authors were not able to determine the exchange rate since the system is too reactive. By employing isotopic labeling studied by NMR and using the reasoning described above, in this current study it was however possible to do a more accurate analysis of the Mo(IV) system. Since there is a factor of *ca.* 300 difference between the complex formation results for the $[MoO(OH_2)(CN)_4]^{2-}$ compared to the W(IV) complex, and all experimental results to date indicate that these substitution reactions of the aqua oxo complex proceed *via* a dissociative mode of activation, an estimate of both values for the oxygen exchange rate constants for the aqua oxo and hydroxo oxo complexes of Mo(IV) can consequently be made, assuming similar relative reactivities. The values for k_{aq} and

k_{OH} for the Mo(IV) center as reported in Table 3 could consequently be estimated.

Technetium(V). The Tc(V) system is, according to the anation results in Table 1, *ca.* 4 orders of magnitude more reactive than the Re(V) system, suggesting that measurable exchange kinetics should be observed at pH values around 8, which proved to be true. Of significance is the fact that no other species (*i.e.*, than that of the dioxo complex) showed any observable contribution to the exchange under the conditions studied (zero intercept). Since it is found that actual exchange of the oxo groups is negligible even in a labile system such as that of the Tc(V) center, it seems fair to assume that it should certainly hold for less reactive systems such as that of Re(V) and W(IV), as mentioned above.

A limitation encountered in the Tc(V) system is the fact that the rate constant for the water exchange of the $[TcO(OH_2)(CN)_4]^-$ complex, k_{aq}, could not be determined as a result of the reactivity of the system. Since the pK_{a2} value of the Tc(V) aqua oxo complex is not accurately known, a similar uncertainty exists in the true value of k_{OH}. The slope of the line in Figure 4 ($=k_{OH}/K_{a2}$) can however be accurately determined. In spite of the uncertainty in the k_{OH} value for the Tc(V) system, the high reactivity when compared to that of the Re(V) is still worth noting, as mentioned in our previous studies. This fact, as reported earlier, has significant consequences for the preparation and *in vivo* behavior of Re analogs to existing Tc(V) diagnostic radiopharmaceuticals. The relative kinetic reactivity, for example, in the washout of a Re(V) complex from the human system at blood pH values (*ca.* 7) via an exchange type of mechanism can be calculated. Directly based on the results obtained in this study the observed exchange constant for a Re(V) complex at 25 °C will be 8.9×10^{-7} s^{-1} compared to that in the Tc(V) system of 2.3×10^{-2} s^{-1}, *ca.* 26 000 times slower. In real terms this reduces to a 30 s reaction for Tc(V) compared to 9 days for the Re(V) system.

Mechanism of Oxygen Exchange. In the Re(V) and W(IV) aqua oxo complexes comparison of both the complex formation of the $[MO(OH_2)(CN)_4]^{n-}$ by NCS^- ions and the water exchange (k_{aq}) shows a relative increase in reactivity of approximately 3 orders of magnitude (Tables 1 and 3), which is in direct agreement with the previously[3,4] concluded dissociative activation. The increase in Lewis acidity of the Re(V) center compared to that of W(IV) will result in a much less reactive system in a dissociatively activated mode. The activation entropies determined for both these systems are in general agreement with a *d*-activation. The above mentioned ground state distortion from the normal octahedral geometry, *i.e.*, the displacement of the central metal atom by up to 0.35 Å toward the oxo from the plane formed by the four cyano carbon atoms, is in agreement with this reasoning. Furthermore, the determination of the volume of activation of +10.6 cm^3 mol^{-1} for the anation of the $[WO(OH_2)(CN)_4]^{2-}$ complex by N_3^- ions[4,14] provides strong evidence in favor of a dissociative mode of activation in the aqua oxo complexes.

Evaluation of the relative reactivity of the $[MO(OH)(CN)_4]^{(n+1)-}$ complexes for the Re(V) and W(IV) metal centers reveals an interesting observation, *i.e.*, that the rate of exchange of the Re(V) hydroxo oxo complex, when compared to that of the W(IV), shows a 5-fold *increase* in reaction rate compared to the 3 order of magnitude *decrease* for the aqua complexes as described above. This, together with the fact that the activation entropy for k_{OH} for both the complexes (Table 3), which shows a tendency toward negative values, might be interpreted as evidence in favor of a less dissociative or even of an associative type of mechanism being operative for the oxygen exchange in the hydroxo oxo complexes. This reasoning is in line with the ground state properties that are available.[3,4] For example, the distortion in the $[ReO(OH)(CN)_4]^{2-}$ and the $[MoO(OH)(CN)_4]^{3-}$ complexes as manifested in the displacement of the central metal atom toward the oxo from the plane formed by the four cyano carbon atoms is only ca. 0.15 Å compared to up to 0.35 Å for the aqua oxo complexes as mentioned above. The NC−M−OH bond angles are around 85−87° whereas those of the NC−M−OH_2 are only ca. 80°. This consequent decrease of the steric repulsion exerted by the cyano ligands in the hydroxo oxo complex implies less interaction with both the leaving and entering ligand in the probable region of attack. Furthermore, the M−OH bonds in the $[MoO(OH)(CN)_4]^{3-}$ and $[ReO(OH)(CN)_4]^{3-}$ complexes are ca. 0.24−0.42 Å *shorter* than the corresponding M−OH_2 bonds in the aqua oxo complexes and are therefore obviously much stronger. This clearly suggests that the hydroxo ligand in these 16 electron complexes will dissociate with much more difficulty and suggests that association might indeed be favored.

The difference between the oxygen exchange rate in the aqua oxo complex compared to that of the hydroxo oxo (k_{aq} and k_{OH} in Table 3) for the W(IV) center is *ca.* 5 orders of magnitude but only 27 times for the Re(V). This large relative increase in the reactivity of the W(IV) hydroxo complex compared to the Re(V) is further evidence pointing to the importance of association in the oxygen exchange on the hydroxo complexes.

Upon comparison of the k_{OH} exchange rate of the Tc(V) system with that of the Re(V), the significant increase in reactivity (ca. 3 orders of magnitude) is still very prominent and not necessarily indicative of an associative activation. It is however possible that the Tc(V) hydroxo complex might be very reactive via an associative pathway, since it is known that the Tc(V) center much more readily accepts electron density than does the corresponding Re(V) complexes.[15] The greater ease by which coordination sphere expansion can occur in third-row d series transition elements such as W(IV) and Re(V) (not very easily accomplished in the second-row, *i.e.*, for Tc) furthermore favors an oxygen exchange process *via* a more associative pathway for the hydroxo oxo complexes. Further studies in this regard, which will include high-pressure investigations, are planned in order to present more details on the substitution and exchange behavior of these hydroxo systems.

Oxygen *vs* Proton Exchange. On the basis of previous studies, the question as to possible interdependence of oxygen and proton exchange reactions in terms of observations made by ^{17}O NMR was raised. To determine this it is however necessary to note all the actual rate-determining processes applicable, i.e., that of both the oxygen and the proton exchange as a function of pH. It was shown from the previous line-broadening study[7] that the characteristics of the oxygen-17 NMR signals in these complexes are governed by the concentration of the dioxo complex, acting as "bottleneck" for the systems going into the fast/slow exchange regimes, which in turn depended primarily on the pH and the proton exchange. In the following paragraphs an attempt is being made to correlate these processes with the knowledge available to date on these four metal centers. The inversion rate constants as well as the oxygen exchange rate constants in the under mentioned discussion are available as supplementary material.

(14) Leipoldt, J. G.; van Eldik, R.; Basson, S. S.; Roodt, A. *Inorg. Chem.* **1986**, *25*, 4639.

(15) Tisato, F.; Mazzi, U.; Bandoli, G.; Cros, G.; Darbieu, M.; Coulais, Y.; Guiraudi, R. *J. Chem. Soc., Dalton Trans.* **1991**, 1301.

Tungsten(IV) and Molybdenum(IV). The dioxo complexes for W(IV) and Mo(IV), having high pK_a values, are formed *via* hydrolysis as the rate-determining step as shown in eq 17 (see

$$\mathrm{OMOH} + \mathrm{OH}^- \underset{k_{2b}}{\overset{k_{-2b}}{\rightleftharpoons}} \mathrm{OMO} + \mathrm{H_2O} \qquad (17)$$

also Scheme 2). In the above mentioned study[7] it was shown that the enrichment of the oxo sites in the hydroxo oxo and aqua oxo complexes is observed as a consequence of the rapid protonation/deprotonation reactions. In the hydroxo oxo and aqua oxo complexes, the significant distortion from octahedral geometry was pointed out earlier (a displacement of the central metal atom up to 0.35 Å toward the oxo from the plane formed by the four cyano ligand carbon atoms). Since the observed rate of enrichment of the oxo in $[MO(OH_2)(CN)_4]^-$ and $[MO(OH)(CN)_4]^{2-}$ is directly coupled to the rate of protonation, i.e., the rate of formation of the dioxo species, it is therefore also directly related to the rate of oscillation of the metal center along the oxo/hydroxo axis, *i.e.*, the rate of inversion (k_{inv}, eq 18) of the protonated species. It has to be noted that a complex

$$\mathrm{d[OMO]/[M]d}t = 2k_{inv} \qquad (18)$$

however statistically inverts at half the rate of formation of the dioxo complex, resulting in eq 18. The formation rate of the dioxo species according to eq 17 is given by eq 19. From the

$$\mathrm{d[OMO]/d}t = k_{-2b}[\mathrm{OMOH}][\mathrm{OH}^-] \qquad (19)$$

definition of $K_w = K_{a2}K_{b2} = K_{a2}k_{2b}/k_{-2b}$, eqs 18 and 19, the expression for the rate of oscillation of the metal center along the oxo/hydroxo axis, *i.e.*, the observed inversion rate constant in eq 20, is obtained. The calculated functions for both the

$$k_{inv} = (k_{2b}K_{a2}K_{a1})/2[\mathrm{H}^+]^2/(1 + K_{a1}/[\mathrm{H}^+] + K_{a1}K_{a2}/[\mathrm{H}^+]^2) \qquad (20)$$

observed inversion rate constant (eq 20, line BB′, rate constants Table 4) and the observed intermolecular oxygen exchange rate constant (eq 12, line AA′) as a function of pH for the W(IV) system are illustrated in Figure 6a. On the figure is also given the simplified expressions for the observed rate constants as defined by the two functions. The data points obtained experimentally, available as supplementary material, are also shown. The data points D were calculated from the line broadening on the coalesced signal as the system exits the fast exchange regime with respect to proton exchange, while those at point E were obtained from the line broadening observed on the oxo signal of the $[WO(OH_2)(CN)_4]^{2-}$ complex. (Below pH *ca.* 10 both the oxo and aqua/hydroxo signals were observed, indicative of the slow exchange with regard to the proton transfer.) The slower intermolecular oxygen exchange data (illustrated in Figure 2) are shown at G. The two functions intersect at C.

A very significant observation can be made from the results illustrated in Figure 6a. From C to A′ and C to B′ it is clear that the inversion rate is more rapid than the oxygen exchange, *i.e.*, the growth of the ^{17}O signal *vs* time. The actual oxygen exchange process is observed by conventional isotopic exchange. However, once C is reached, when moving to lower pH, the oxygen exchange at the aqua ligand of the $[WO(OH_2)(CN)_4]^{2-}$ complex becomes *more rapid* than the proton exchange, while the signal increase of the oxo signal *vs* time now gives the *proton* transfer process which defines k_{inv}. This was confirmed experimentally as follows: (i) The data points at F were obtained by monitoring the isotopic exchange of the *oxo* signal

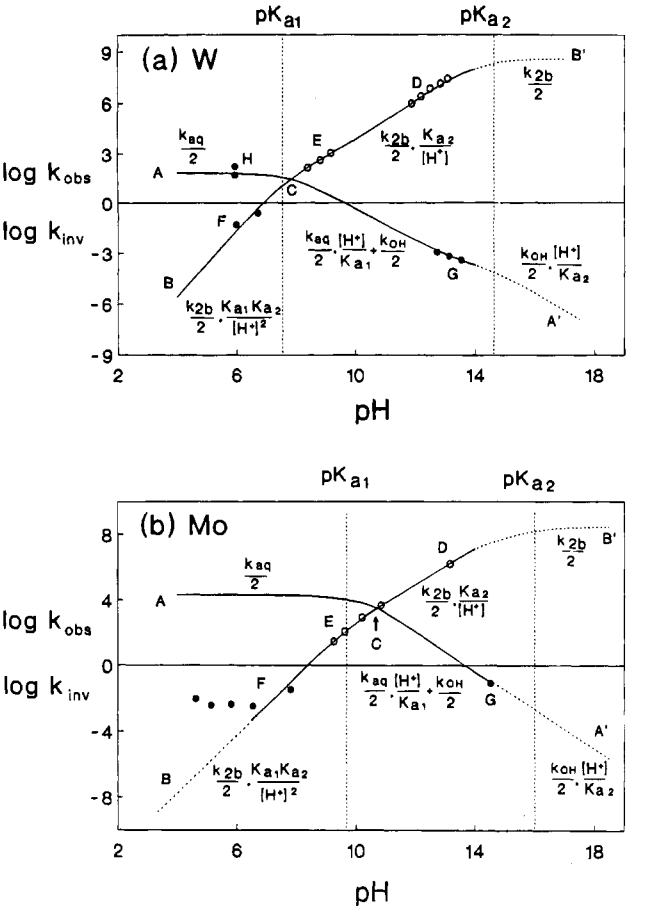

Figure 6. Inversion and oxygen exchange rate as a function of pH for (a) W(IV) and (b) Mo(IV), at 25 °C, data points illustrating pH range studied. Line AA′ calculated from eq 12 gives observed oxygen exchange. Line BB′ calculated from eq 20 gives the observed inversion rate. Regions where appropriate equations can be simplified are shown. Open and solid circles represent the line-broadening and isotopic exchange data points, respectively.

(of the $[WO(OH_2)(CN)_4]^{2-}$ complex, δ = 751 ppm) increase *vs* time at lower pH values (Table 4), thus clearly showing the oxygen exchange thereupon is determined by the proton exchange (eq 19). (ii) Data points H were obtained (as estimated limits) by a variable-temperature line-broadening study (Table 5, text above) of the *aqua* signal (δ = −15 ppm), confirming the aqua exchange to be much more rapid than the effective proton transfer as observed by the enrichment of the oxo signal.

The above reasoning also holds for the Mo(IV) center in Figure 6b, *i.e.*, in the two functions for the observed intermolecular oxygen (eq 12) and the inversion (eq 22) rates, respectively, illustrating the different processes. For the calculation of line AA′ in Figure 6b the estimated values of 4.1×10^4 s^{-1} for k_{aq} and 0.2 s^{-1} for k_{OH} (Table 3) were used, since this could not be determined experimentally due to the high reactivity of the system. The one data point obtained at $[OH^-]$ = 5 M (G in Figure 6b) is in very good agreement with the function. Again, as shown for the W(IV) center, the inversion rate constants shown in Figure 6b at D (fast exchange region) and E (slow exchange) were obtained from the line-broadening study. In this case, no *aqua* signal was observed since, as a result of the high reactivity of the Mo(IV), the coordinated aqua is in fast exchange with the bulk water. As in the case of the W(IV) mentioned above, the slow exchange of the oxo of the $[MoO(OH_2)(CN)_4]^{2-}$ complex was also monitored a pH of 7.5, confirming eq 19 as valid for describing the proton exchange up to this acidity. However, as soon as the pH was lowered

further, the proton exchange became acid independent (F in Figure 6b). A possible explanation of this behavior might be linked to the protonation of the oxo ligand in $[MoO(OH_2)(CN)_4]^-$, yielding small quantities of intermediate dihydroxo species for the inversion process, as has been postulated to exist previously.[16]

Rhenium(V) and Technetium(V). Reasoning similar to that above holds for these two systems. The formation of the dioxo complex as the rate-determining step in Scheme 2 is in this case given by the protolysis reaction in eq 21. The inversion

$$\mathrm{OMOH} \underset{k_{-2a}}{\overset{k_{2a}}{\rightleftharpoons}} \mathrm{OMO} + \mathrm{H}^+ \qquad (21)$$

rate constant of the protonated species, as described above, is given by eq 18. The formation rate of the dioxo complex for the Re(V) and Tc(V) systems (lower pK_a values) is given by eq 22. Substituting eqs 18 and 22, the observed rate of proton

$$\mathrm{d[OMO]}/\mathrm{d}t = k_{2a}[\mathrm{OMOH}] \qquad (22)$$

transfer/oscillation of the metal center along the oxo/hydroxo axis, k_{inv}, as given by eq 23, is obtained. Upon introduction of

$$k_{inv} = (k_{2a}K_{a2}/2[\mathrm{H}^+])/[(1 + K_{a1}/[\mathrm{H}^+] + K_{a1}K_{a2}/[\mathrm{H}^+]^2)] \qquad (23)$$

the data in Tables 1 and 3 in eqs 12 and 23, the dependence of the observed intermolecular oxygen exchange (line AA′) and the inversion rate (line BB′) for the Re(V) system, as shown in Figure 7a, is obtained. The difference in the illustrated observed inversion rate (line BB′) as compared to the W(IV) and Mo(IV) described above stems from the fact that different mechanisms holds for the proton exchange in these systems (eqs 17 and 21, as has been shown previously). The experimental data points for both the oxygen and the proton exchange are in good agreement with the calculated functions (line-broadening results D, oxygen exchange E). It is clear from Figure 7a that, as in the case of the above mentioned W(IV) and Mo(IV) systems, a (theoretical, pH *ca.* −6!) point C is reached where the increase in the observed exchange at the oxo peak in the $[ReO(OH_2)(CN)_4]^-$ complex is determined by the proton transfer. In this case it is however just of theoretical relevance since that acid concentration is not accessible.

Similar to the Re(V) system, the observed intermolecular oxygen exchange and the rate of inversion as a function of pH of the Tc(V) is compared in Figure 7b. The experimental results are again in agreement with the theoretical functions (the line-broadening results at D, oxygen exchange E). The two functions converge at a point C which is, as in the case of the Re(V) system, just of theoretical relevance.

To conclude, in this study we have shown that it was possible with oxygen-17 NMR to successfully study the slow intermolecular oxygen exchange in these oxo cyano complexes. We have furthermore correlated the oxygen exchange with the previous proton transfer kinetic study and showed the interdependence between the proton transfer and the actual dynamic inversion of the metal center. Of special significance is the fact that we were able to study different kinetic aspects of these complexes spanning up to 10 orders of magnitude—indeed a wide range! An important result from this study concerns specifically the oxygen exchange in oxo complexes. It has to be underlined that observed oxygen exchange has to be interpreted with care since there might be preceding (i.e., protonation) rate-determining steps governing the actual oxygen exchange.

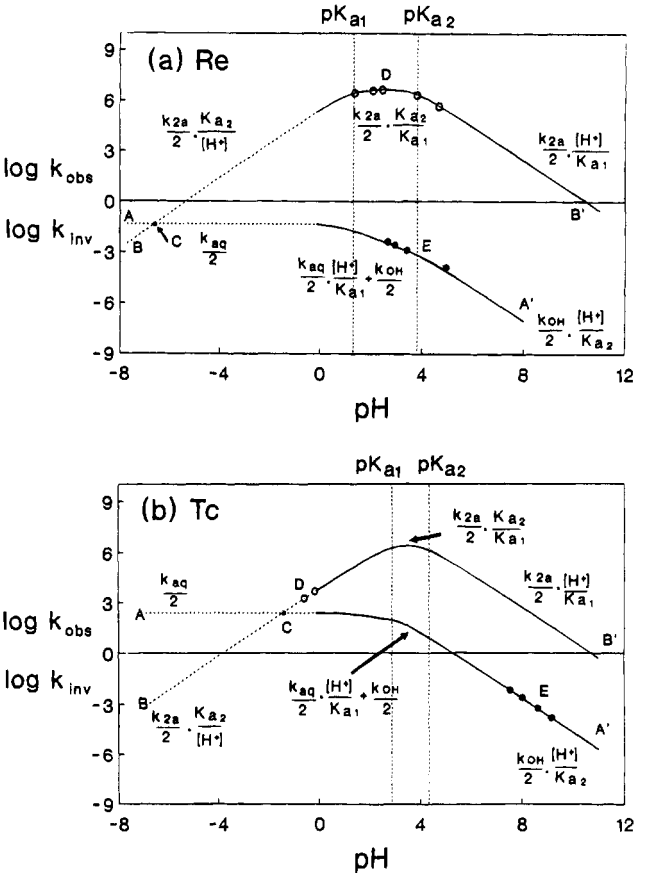

Figure 7. Inversion and oxygen exchange rate as a function of pH for (a) Re(V) and (b) Tc(V), at 25 °C, data points illustrating pH range studied. Line AA′ calculated from eq 12 gives observed oxygen exchange. Line BB′ calculated from eq 23 gives observed inversion rate. Regions where appropriate equations can be simplified are shown. Open and solid circles represent the line-broadening and isotopic exchange data points, respectively.

Acknowledgment. Financial support for this research, provided by the Swiss National Science Foundation (Grant No. 2039483.93), is gratefully acknowledged. A.R. and J.G.L. also thank the Research Fund of the University of the Orange Free State and the South African FRD for financial assistance.

Supplementary Material Available: Tables of the observed rate constants for the slow isotopic ^{17}O exchange as well as the calculated inversion rates (2 pages). Ordering information is given on any current masthead page.

IC9406603

(16) Van de Poel, J.; Neumann, H. M. *Inorg. Chem.* **1968**, *7*, 2086.